

Article

## The Effect of CFRP Length on the Failure Mode of Strengthened Concrete Beams

Jun Ding <sup>1,\*</sup>, Fang Wang <sup>2</sup>, Xia Huang <sup>1</sup> and Song Chen <sup>1</sup>

<sup>1</sup> College of Mechanical Engineering, Chongqing University of Technology, Chongqing 400054, China; E-Mails: huangxia@cqut.edu.cn (X.H.); songchen1133@163.com (S.C.)

<sup>2</sup> School of Materials Science and Engineering, Southwest University, Chongqing 400715, China; E-Mail: wangfang\_cq1978@163.com

\* Author to whom correspondence should be addressed; E-Mail: dingjunawen@126.com; Tel./Fax: +86-023-625-630-39.

Received: 9 April 2014; in revised form: 30 May 2014 / Accepted: 3 June 2014 /

Published: 10 June 2014

---

**Abstract:** This paper reports the effects of carbon fiber-reinforced polymer (CFRP) length on the failure process, pattern and crack propagation for a strengthened concrete beam with an initial notch. The experiments measuring load-bearing capacity for concrete beams with various CFRP lengths have been performed, wherein the crack opening displacements (COD) at the initial notch are also measured. The application of CFRP can significantly improve the load-bearing capacity, and the failure modes seem different with various CFRP lengths. The stress profiles in the concrete material around the crack tip, at the end of CFRP and at the interface between the concrete and CFRP are then calculated using the finite element method. The experiment measurements are validated by theoretical derivation and also support the finite element analysis. The results show that CFRP can significantly increase the ultimate load of the beam, while such an increase stops as the length reaches 0.15 m. It is also concluded that the CFRP length can influence the stress distribution at three critical stress regions for strengthened concrete beams. However, the optimum CFRP lengths vary with different critical stress regions. For the region around the crack tip, it is 0.15 m; for the region at the interface it is 0.25 m, and for the region at the end of CFRP, it is 0.30 m. In conclusion, the optimum CFRP length in this work is 0.30 m, at which CFRP strengthening is fully functioning, which thus provides a good reference for the retrofitting of buildings.

**Keywords:** carbon fiber-reinforced polymer (CFRP) length; failure mode; finite element method; strengthened concrete beams

---

## 1. Introduction

The applications of carbon fiber-reinforced polymer (CFRP) for strengthening concrete structures have recently received considerable attention. Various methods are extensively used for strengthening concrete structures, especially for flexural members; these methods include the use of additional steel parts, external pre-stressing of parts and reducing or bridging the gap between supports [1–4]. However, these methods generally require considerable economic cost and consume a great deal of time. By contrast, CFRP is high in strength and rigidity, as well as having a low specific weight. Thus, this material has widely been applied in structural engineering for the retrofitting and strengthening of reinforced concrete (RC) beams and steel beams (both of them are similar in flexural behavior).

A review of previous studies shows that CFRP is normally bonded onto the bottom side of flexural members (or the tension area) to improve the bending resistance and shear performance of the RC beams and steel beams. Edberg *et al.* [5] presented an experimental study in which five different configurations of glass and CFRP were attached to the tensile flange of small-scale RC beams using adhesive. Buyle-Bodin *et al.* [6] investigated the flexural behavior of RC beams externally reinforced using CFRP and performed nonlinear finite element analysis to complete the experimental analysis of the beams. Mazzotti *et al.* [7] conducted the experimental observation for studying on the delamination of RC beams bonded FRP plates. Martinez *et al.* [8] employed serial/parallel mixing theory into finite element procedures to numerically simulate RC structures reinforced with FRP. In addition, Tavakkolizadeh [9] tested small-scale steel beams in four-point bending. The research [10,11] demonstrated that the cracking moment in reinforced concrete beams with CFRP may increase from 12% to 230%. All of these aforementioned studies showed that concrete beams can feasibly and significantly strengthen flexural capacity by using CFRP plates. Once the sustainable load on the tensile concrete beam increases up to some value, the concrete beam is often damaged, because of the failure at the interface between the concrete beam and CFRP or because of debonding at the end of the CFRP. The predication and identification of CFRP failure modes in the flexural strengthening of concrete beams are useful for overcoming or arresting these failures. Deng *et al.* [12] highlighted an important feature of the steel beam, that is, the stress concentration on the adhesive at the tip of the CFRP plate, because of the abrupt termination of the CFRP plate. Buyukozturk *et al.* [13] reviewed their achievements and concluded that failures of CFRP flexurally-strengthened RC beams and steel members occur because of different mechanisms that strongly depend on the strengthening parameters. Shear failure was found to occur when the shear capacity of the beam cannot accommodate the increment of flexural capacity, because of flexural strengthening. The buckling in compression, CFRP rupture and debonding of CFRP are specified as the major failure modes of concrete beams strengthened with CFRP. Schnerch *et al.* [14,15] investigated the flexural strengthening of steel beams using CFRP. They focused on steel structures with FRP because of the lack of information for steel structures with FRP as compared with concrete structures with FRP. They found that the bonding

behavior of CFRP to the concrete beam completely differs from that of steel members in terms of failure modes. A higher bonding stress was found to have developed in the adhesive for steel members than for concrete beams. The delamination failure of flexurally-strengthened steel beams with externally-bonded CFRP was investigated by Colombi *et al.* [16] in which the simplified fracture mechanics approach was employed to investigate edge delamination. Belachour *et al.* [17] derived the analytical solution for interfacial stress in the case of simply supported beams strengthened with prestressed CFRP plates. The solution shows that a high concentration of both shear and normal stresses occurred at the ends of the CFRP, thus resulting in the premature failure of the strengthened specimens at these locations. Al-Emarani *et al.* [18] experimentally investigated the effect of strengthening steel beams in flexure with short-length CFRP with different anchorage systems. The result shows that a reduction in the CFRP plate length will result in an overall cost reduction of the CFRP strengthening alternative. Additionally, the load carrying capacity of the RC beams can be significantly improved with a shorter length of CFRP plates if strengthened beams are properly anchored with devices. To investigate further the strengthening effect of CFRP on the loading capacity of the beams, the primary focus was on both experimental measurement and numerical simulation. Several numerical programs and simulation procedures have been developed to examine the performance of RC beams strengthened with CFRP plates through finite element (FE) simulation. Lu *et al.* [19] developed a meso-scale numerical model to predict the debonding process in FRP-concrete bonded joints using the fixed angle crack model employed in a very fine mesh size, and the result showed good agreement with experimental observation. Atas *et al.* [20] developed a 3D FE model and used cohesive elements to predict the debonding phenomenon of different strengthening systems. Chen *et al.* [21] investigated the effects of various modeling assumptions on the interfaces between concrete, main steel bars and shear stirrups, as well as between concrete and FRP on the shear performance of strengthened RC beams.

However, a review of previous works shows that limited information has focused on the in-depth exploration of the effect of the CFRP length attached on beams. No study has investigated pre-existing cracked beams under tensile loading with various CFRP lengths. Damaged bridges or RC beams require immediate repair in structural engineering. The amount of damage or the length of CFRP-bonded beams depends on the timely strengthening effect during retrofitting. Our previous works [22–24] show that the influence of the initial crack length (in the form of a notch) is only obvious at the regional stress field near the initial crack tip, but is negligible at the overstressed region of the carbon fiber plate, as well as at the interface between the carbon fiber plate and concrete. Moreover, the initial crack propagation stops after reaching a certain length. Consequently, the eventual failure of the carbon fiber-RC beam occurs because of the appearance of new cracks on the concrete section at the bottom of the reinforced beam or because of the penetration between cracks rather than the propagation of the Type I crack at the end of the notch. Thus, the effect of the length of the carbon fiber plate on the failure process of RC specimens must be studied.

This research aims to investigate numerically the effect of CFRP length on three critical stress areas in strengthened beams. The concrete beams used in this work exhibit a pre-existing 20 mm-long crack (notch) located in the middle. The effects of CFRP length on the stress fields at the initial crack, at the interface between CFRP and the concrete beam, as well as at the end of the CFRP next to the concrete beam side have been carefully explored using the FE method. The result shows that the major factor

contributing to the strengthening effect for concrete beams depends on the CFRP length. For a certain length, the stress at the initial crack seems rather reasonable, even under the relatively large magnitude of the load. The various lengths of CFRP also had an obvious effect on the failure modes of strengthened beams. The experimental observations also support this finding and can serve as a good reference for repairing some damaged members in structural engineering.

## 2. Materials and Methods

### 2.1. Materials

Concrete is a composite composed of coarse granular materials embedded in a hard matrix of cement that fills the space between aggregate particles and glues them together. Considering both the cost of construction and the generality of the experiment, a concrete material (marked as C30) typically used in the construction industry was employed to make the concrete beams with the specific composition shown in Table 1. In order to make a concrete block with a higher compressive strength and to improve the pumping performance for concrete, the pumping admixture of the type (Manufactured by Chongqing Chuanqing Chemical Plant, Chongqing, China), was used in the concrete mix design. The cement was an ordinary Portland one belonging to the strength class, 42.5 R. The mud contents for the fine and coarse aggregates are 3.0% and 5.0%, respectively. For better characterizing the used concrete, a slump test was firstly conducted on fresh concrete made according to the mix proportion (Table 1) to investigate the workability of the concrete, ensuring successful operation in the construction of concrete beams. Then, the tensile test experiment for measuring the concrete tensile strength was also performed for the concrete specimen, and its tensile strength is about 5.15 MPa. Such a value is much larger than that of commonly used concrete (about 1.53 MPa). However, considering that the tensile strength of concrete accounts for approximately one tenth of the compressive strength for curing length of one month (for this case, the compressive strength with 28 curing days reaches 41.4 MPa), 5.15 MPa of tensile strength for concrete subsequently seems rather reasonable [25]. The ultimate compressive stress for concrete material normally varies with curing days (Table 2). In this work, the concrete beams had been cured at room temperature for 28 days, and the compressive stress was taken at approximately 41.4 MPa for subsequent numerical simulation. The other material properties of concrete are given in Table 3.

**Table 1.** The mix proportion for concrete.

Material	Cement	Coarse aggregate	Fine aggregate	Water	Concrete admixture	Fly-ash
Weight per concrete cubic meter (kg)	300	615	1210	185	6.60	95
Mass ratio	1.000	2.050	4.033	0.617	0.022	0.317

**Table 2.** The ultimate strength variation with curing days.

Curing days	Compressive strength (MPa)
3	23.4
7	29.9
28	41.4

**Table 3.** The material properties for concrete, carbon fiber-reinforced polymer (CFRP) and adhesive.

Material	Concrete	CFRP	Adhesive
Elastic Modulus (GPa)	32.89	165	9.60
Poisson's ratio	0.28	0.25	0.30

CFRP material has a high tensile strength, which can significantly improve the structural behavior of concrete beams. CFRP is normally produced in the form of a strip (plate) or a sheet (wrap). In this research, the adopted CFRP was produced by Taiwan Zhongyi Company, and its typical mechanical behaviors are illustrated in Table 4. The tensile strength is the maximum stress that the CFRP can withstand before it fails, and the ductility refers to its ability to deform tensile stress, equivalent to the rupture strain. They are 4640 MPa and 1.7%, respectively, for the CFRP material [26]. Based on their unidirectional behavior, CFRP plates are grouped into orthotropic materials and are made in different lengths and thicknesses, as required. The material properties of CFRP generally depend on the geometric dimensions, including the thickness and length. However, considering that the change in length and thickness of CFRP is minor and that the strengthened beam sustains mostly bending loading, the isotropic material behavior for CFRP is considered without loss of generality. The other material properties for CFRP are summarized in Table 3.

To transfer the interfacial stress sufficiently from the concrete beam to the CFRP plates, a typical engineering resin with a strong bond strength that is widely applied in structural engineering is employed. The adhesive is a two-part epoxy resin (resin and hardener in 3:1 proportions) that must be mixed with 1% by weight of ballotini (1 mm diameter) to ensure the uniform thickness of the bond line. Table 3 shows the elastic modulus and Poisson's ratio of the used adhesive.

**Table 4.** The typical mechanical parameters for CFRP.

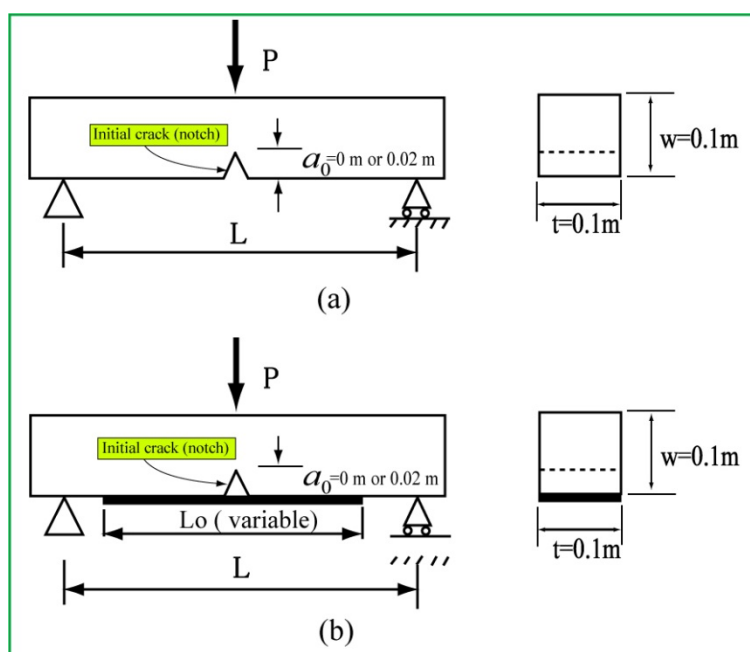
Density	Tensile strength	Ductility	Typical thickness
20 g·m <sup>-3</sup>	4640 MPa	1.7%	0.111 mm

## 2.2. Specifications of the Beams

To investigate the effects of CFRP length on failure behavior in terms of stresses at three critical areas, different lengths of CFRP at 0.10 m, 0.15 m, 0.20 m, 0.25 m, 0.30 m and 0.35 m are employed for external bonding at the bottom of concrete beams for strengthening. The concrete beams are divided into two groups, one with a notch of 20 mm and the other without a notch, to investigate the effect on the failure process for beams. The notch located at the midpoint of the beam was made by placing a wedge-shaped object inside the midpoint of the beam when the concrete beams were constructed. The notch indicates the existence of defects or faults, which significantly decrease the

bending stiffness of beams. Plain concrete beams were used in this research, indicating that no reinforced steel bars are employed to strengthen a concrete beam. Although plain concrete beams are rarely used for support as flexure members, this research aims to investigate the influence of CFRP on the failure process of overall concrete beams, unrelated to steel bars. The geometric dimension for the concrete beams (notched and without notched) is 0.10 m  $\times$  0.10 m  $\times$  0.40 m. The geometric configuration of a concrete beam strengthened with CFRP is illustrated in Figure 1.

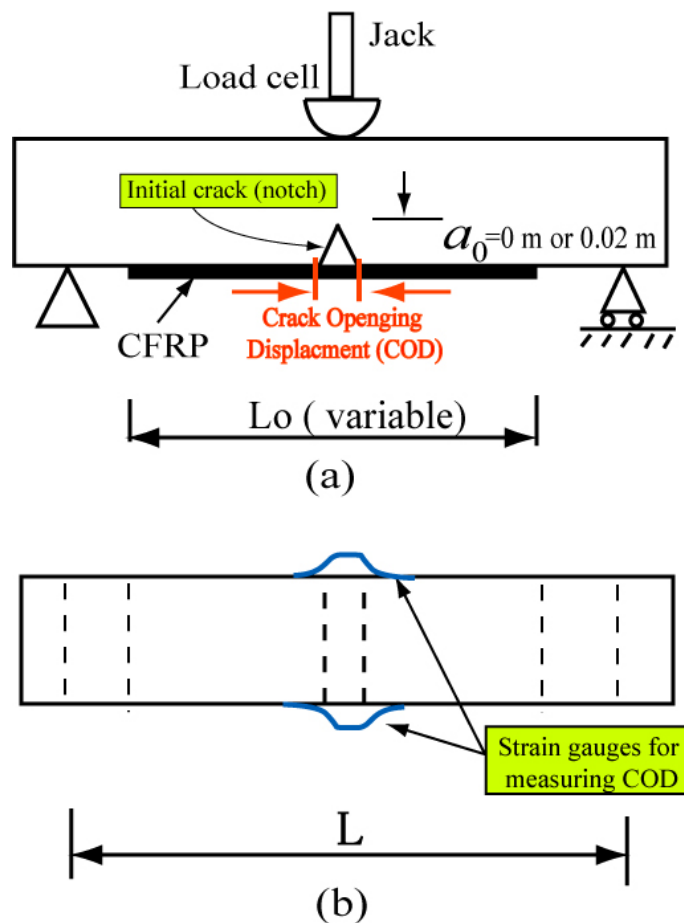
**Figure 1.** The geometrical configuration for a concrete beam: (a) a concrete beam without CFRP; and (b) a concrete beam with CFRP.



### 2.3. Test Setup

The experimental setup is based on a three-point bending test. Since the objective in this research is to investigate the failure process affected by the length of CFRP bonded at the bottom of concrete beams, the load-bearing capacity and the crack opening displacement (COD) measured at the initial notch of the concrete beam are chosen as two major factors. No matter how the failure modes, such as Type I crack propagation, smeared crack at the root of notch or debonding at the end of CFRP, develop alone or together for the strengthened concrete beam, the changes both in COD and the load can show such failure modes happening in a concrete beam. As illustrated in Figure 2, the load was applied to the midpoint of the concrete beam by using a hydraulic jack. The middle of the beam was subjected to jack pressure. Two roller supports carried the reactions, such that the loading was at three incremental bending point loads. The values for the ultimate load for the concrete beam can be found from the reader at the instrument. To measure COD at the initial notch, that is, the displacement developed at the initial crack due to the increment of the load, strain gauges are generally applied, attaching to the bottom of the concrete beam for a beam without CFRP or on the surface of the CFRP for a strengthened beam. However, considering the error in making the initial notch and the unevenness of CFRP, two strain gauges are attached to two sides of the concrete beam near the root of the initial notch (Figure 2b). The final values for COD can be calculated by the average between two sides.

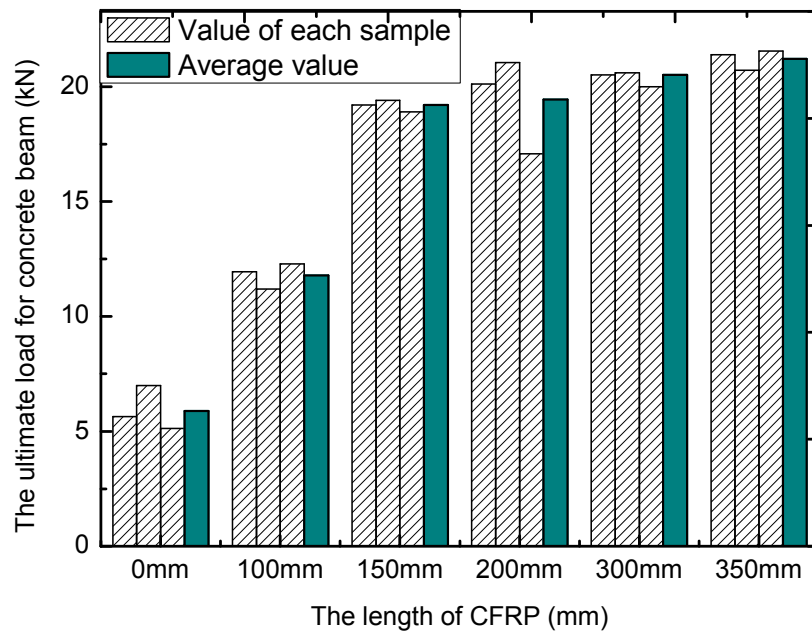
**Figure 2.** The test setup and locations of the strain gauges: (a) test setup; and (b) locations of strain gauges for measuring crack opening displacement (COD).



#### 2.4. Experimental Results

Figure 3 shows the plot of the load-bearing capacity for concrete beams against the various lengths of CFRP, 0 mm (no CFRP strengthened), 100 mm, 150 mm, 200 mm, 300 mm and 350 mm. Each CFRP length corresponds to three concrete specimens, and their experimental results are displayed by oblique line bars. The solid bar represents the average value of every group. It is obvious that the application of CFRP significantly improves the load-bearing capacity (almost a two-times increase in the load compared between the case of 100 mm and the case without CFRP). As the length of CFRP increases, the load-bearing capacity for the strengthened beam also increases, but the increase in the amount of load decreases. When the CFRP length reaches more than 150 mm, the load-bearing capacity for beams remains steady and almost no increase in load occurs, which suggests that the strengthening of CFRP for concrete beams has attained a maximum value.

Figure 3. The plot of load-bearing capacity for concrete beams against the length of CFRP.



In order to validate the accuracy of the experiment measuring the load-bearing capacity, the values for the beams (not CFRP strengthened) with 10 mm, 20 mm and 30 mm of initial notch from experimental measurement and from theory derivation based on fundamental mechanics are compared. In terms of the knowledge of fracture mechanics [27], for a three-point bending specimen with an initial crack, the ultimate load for the beam can be calculated from Formulas (1) and (2).

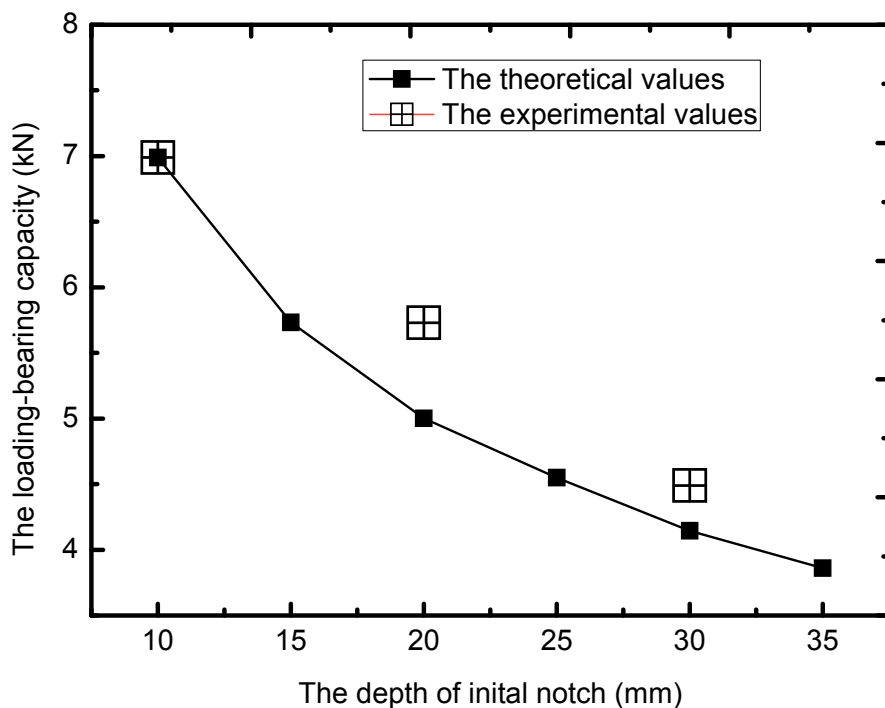
$$K_I = \frac{3SP}{2tW^2} \sqrt{\pi a} F(\alpha) \tag{1}$$

$$F(\alpha) = \frac{1.99 - \alpha(1 - \alpha)(2.15 - 3.93\alpha + 2.7\alpha^2)}{\sqrt{\pi}(1 + 2\alpha)(1 - \alpha)^{3/2}}, \text{ where } \alpha = a / w \tag{2}$$

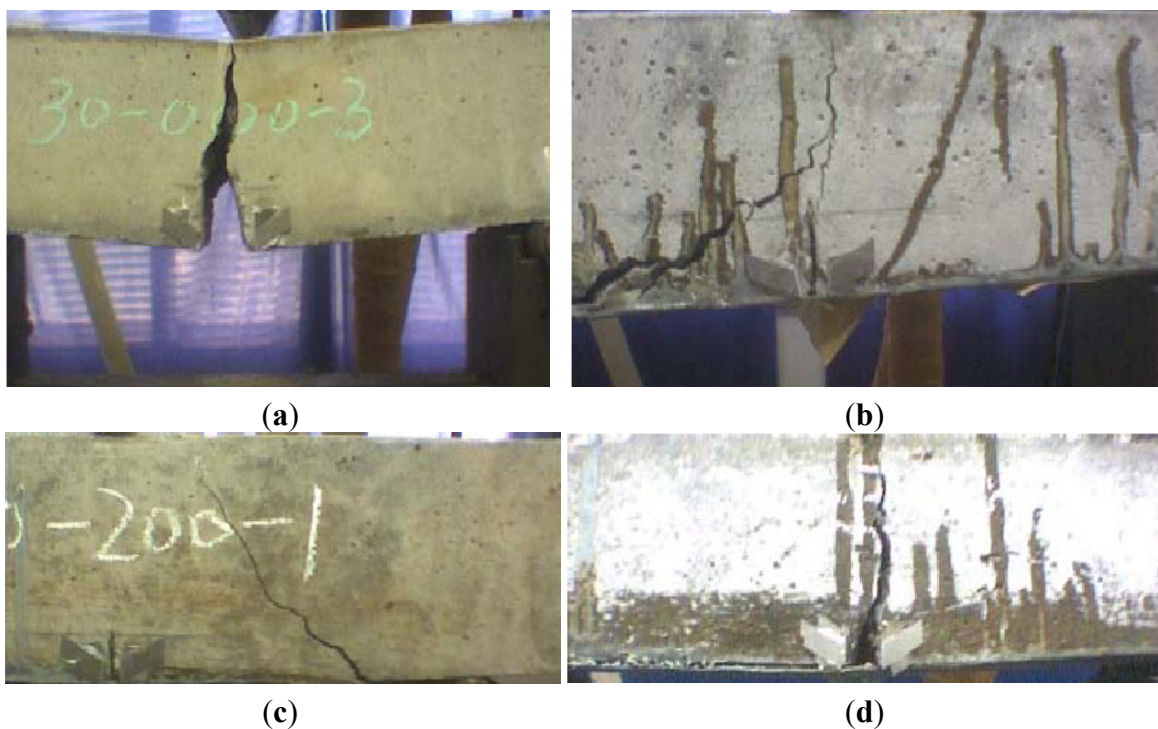
For such concrete beams, the critical stress intensity factor  $K_{IC} = 0.62 \text{ MPa} \cdot \text{m}^{1/2}$ , substituting the geometric dimension and the length of initial notch, the cross air dots in Figure 4 denote the theoretical values for 10 mm, 20 mm and 30 mm, respectively. Additionally, the solid dots represent the values for them from theoretical derivation. It can be seen that they are in good agreement with each other, especially for the case of 10 mm, which indicates the accuracy of the experiment.

Figure 5a shows the failure mode of the concrete beam without CFRP strengthening, whereas Figure 2b–d shows the failure mode of the concrete beam with a CFRP length of 0.10 m, 0.20 m and 0.35 m, respectively. The failure mode for Figure 5a is dominated by Mode I crack propagation along the surface of the initial notch. The inclined crack propagation at an angle of 45° relative to the horizontal axis serves an important function in Figure 5b, along with a minor Mode I crack at the initial notch. For Figure 5c, only an inclined crack with an angle of 45° with respect to a horizontal axis occurs, whereas Mode I crack propagation dominates Figure 5d along with smeared crack propagation at the root of the notch along the interface when the length of CFRP increases to 0.35 m.

**Figure 4.** The comparison of the load-bearing capacity between theoretical and experimental values.



**Figure 5.** The failure mode in experimental observation: (a) failure mode of the beam without CFRP; (b) failure mode of the beam with CFRP of 0.10 m; (c) failure mode of the beam with CFRP of 0.20 m; and (d) failure mode of the beam with CFRP of 0.35 m.

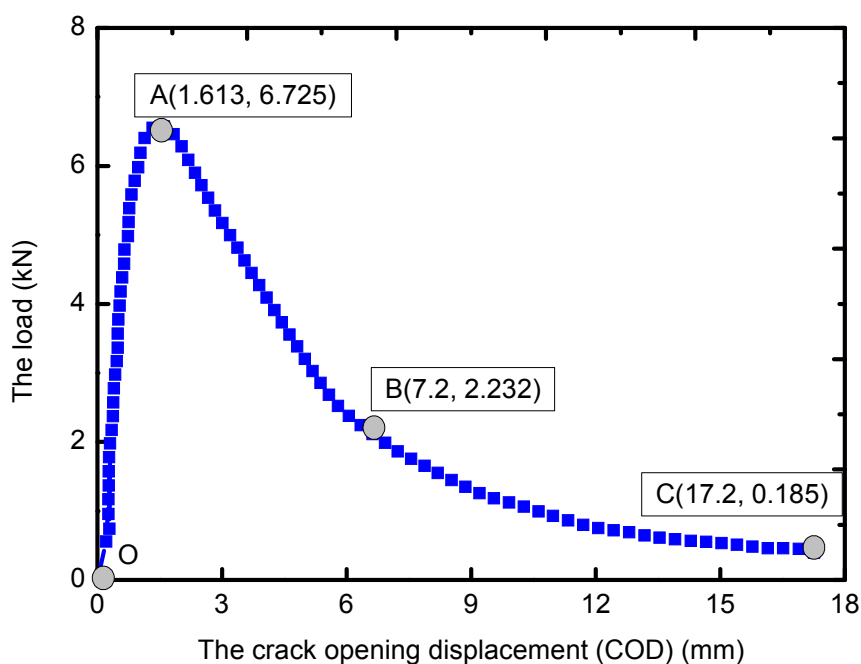


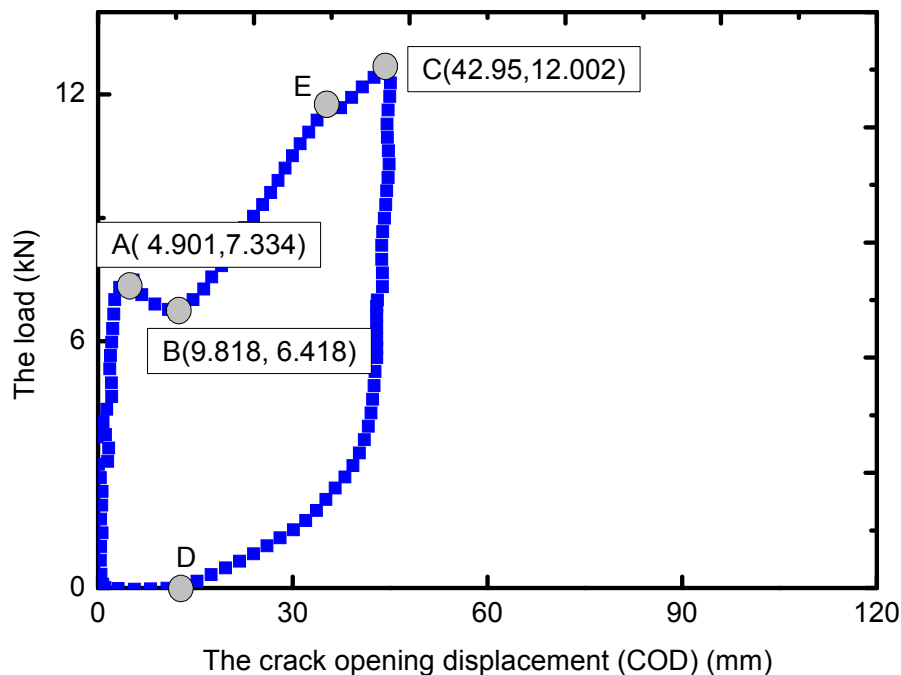
Figures 6 and 7 show the variation of the applied load at the midpoint of the beam with COD for the concrete beam without CFRP and strengthened with CFRP, respectively. The failure modes for the two such cases are different from the experiment. The appearance in both figures can be useful in

supporting such observations. For the case without CFRP strengthening, as the load increases, the concrete beam starts to behave almost elastically, although it includes an initial crack, corresponding to OA in Figure 6. During this period, no new cracks are seen in the concrete beam; subsequently, it can resist the increment in the applied load. The load-bearing capacity reaches a maximum value. After Point A, as the load increases, the micro-cracks initiate at the pre-existed notch and penetrate each other, subsequently reducing the stiffness of the concrete beam, as AB in the figure. As the load continues to increase, the macro-crack quickly propagates and induces Type I mode failure (Point C).

Figure 7 corresponds the case of the concrete beam with CFRP length of 100 mm and its failure mode accounts for Figure 5b. Due to CFRP strengthening, the peak value of the load at Point A seems obviously larger than the case without CFRP, 6.725 kN for the previous one, but 7.334 kN for the latter case. Similarly, after Point A, some cracks are generated in the vicinity of the initial notch, which reduces the load-bearing capacity; slightly decreasing the load seen in Figure 7. In contrast to the previous case, due to the existence of CFRP, as the load increases, the CFRP starts to be stretched to share the load. Subsequently, the concrete beam recovers to the state that resists deformation. Its bearing capacity significantly improves, as seen in BC in Figure 7. After Point C, the stress in concrete material at the end of CFRP reaches the ultimate strength of the concrete and quickly starts to crack with an inclined angle of 45 degree in respect to the horizontal axis. At this time, as a result of constant contact each other between surfaces of initial notch, that is, the initial crack is closed, which results in decrease in COD and then to zero. As the inclined crack (smear crack) at the end of CFRP extends rapidly, the CFRP strengthened concrete beam finally lost the capacity of load-bearing (corresponding to CD line in Figure 7).

**Figure 6.** The variation of load with COD for the concrete beam without CFRP strengthening.

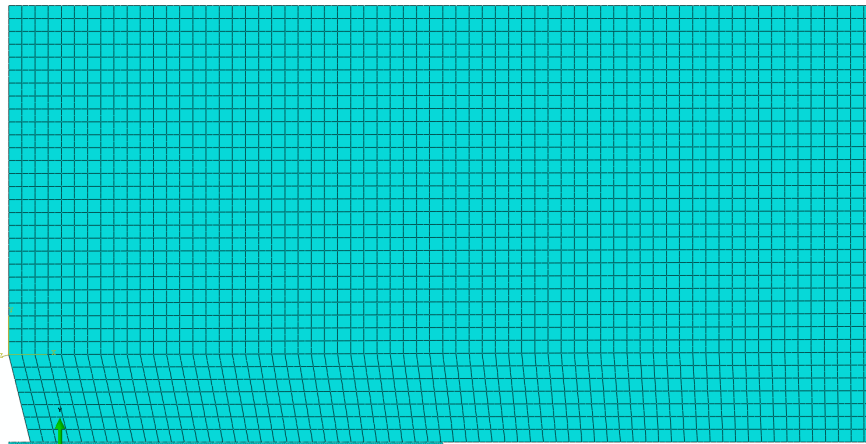


**Figure 7.** The variation of load with COD for the concrete beam with CFRP strengthening.

### 2.5. Numerical Simulation

A two-dimensional FE model was employed to represent the actual geometric configuration of the CFRP-strengthened concrete beam, although this model is a 3D configuration with thickness, because the concrete beam under compressive loading can be simplified as a plane strain state. Figure 8 shows the FE model used for the analysis of the CFRP-strengthened concrete beam. Taking advantage of the geometric symmetry, only half of the specimen was modeled using plane strain elements CPEG4 (4-node bilinear generalized plane strain quadrilateral element) in the ABAQUS software [28]. The FE model consists of 2980 elements, with each node having three degrees of freedom. The elements used to discretize the adhesive layer are considerably smaller than those of both the concrete and CFRP area and are thinner than those at the other areas, because the depth for adhesive is considerably smaller than that for concrete and CFRP. The gap just below the symmetry line represents the notch in the concrete beam (crack), and the area around the notch is also meshed with CPEG4 elements, because no crack extension was simulated in the analysis. To simulate crack extension, two different notch crack initial lengths were used for two separate analyses, whereas all others remain similar, except for the crack length between two FE models. As regards the boundary conditions, the symmetrical boundary condition was applied to the symmetrical line, and only the displacement in the  $y$  direction was constrained for the right node of the beam. This work focuses on the failure of the concrete beam. Thus, considering that concrete is a brittle material, we used the maximum principal stress theory as a criterion to determine whether and when concrete starts to fracture.

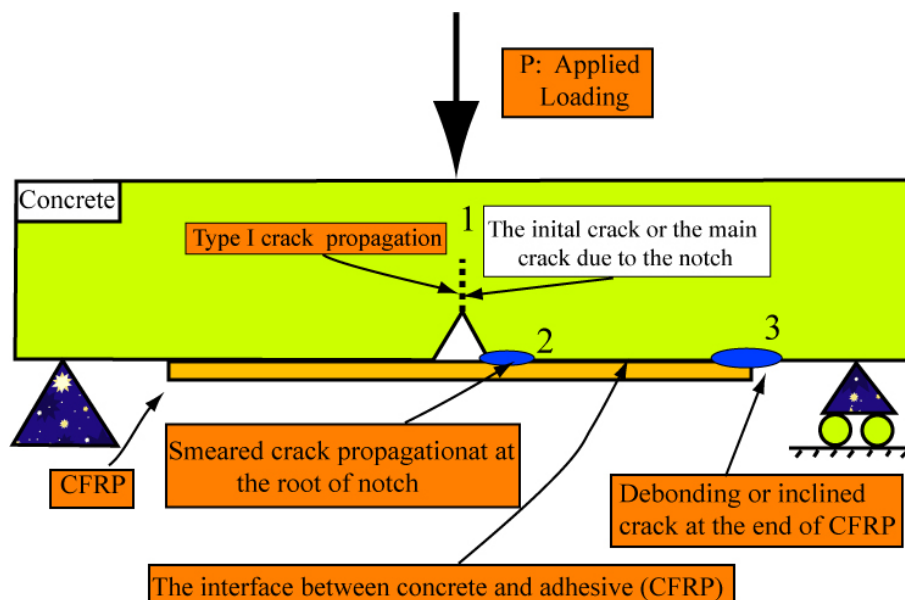
**Figure 8.** The finite element model for a strengthened concrete beam.



### 3. Results and Discussion

A few FE analyses have been performed on strengthened concrete beams based on the previously described geometric configuration and FE model. The investigation on the stress state focuses on three critical regions of the CFRP concrete beam, one located at the initial crack tip (notch), the other at the root of notch along the interface and the third at the end of CFRP, which are marked as 1, 2 and 3 in Figure 9, respectively.

**Figure 9.** The critical stress regions for a CFRP-strengthened concrete beam.



#### 3.1. The Effect of CFRP Length on Stresses around the Crack Tip

Under the condition of concentrated load in three-point bending, the CFRP-strengthened concrete beam will produce an overstressed region in which the maximum principal stress is larger than the tensile strength of the concrete at the notch tip. In this section, the influence of the CFRP length on the overstressed region at the notch tip was investigated. The maximum principal stresses at the notch tip were calculated using FEM when the length of CFRP is 0 m, 0.10 m, 0.15 m, 0.20 m, 0.25 m, 0.30 m,

and 0.35 m for 0 m and 0.02 m notch lengths under 20 kN loading. Figure 10 illustrates the variation of the maximum principal stress at the notch tip with the length of CFRP bonded onto the concrete beam.

**Figure 10.** The plot of maximum principle stress against the length of CFRP.

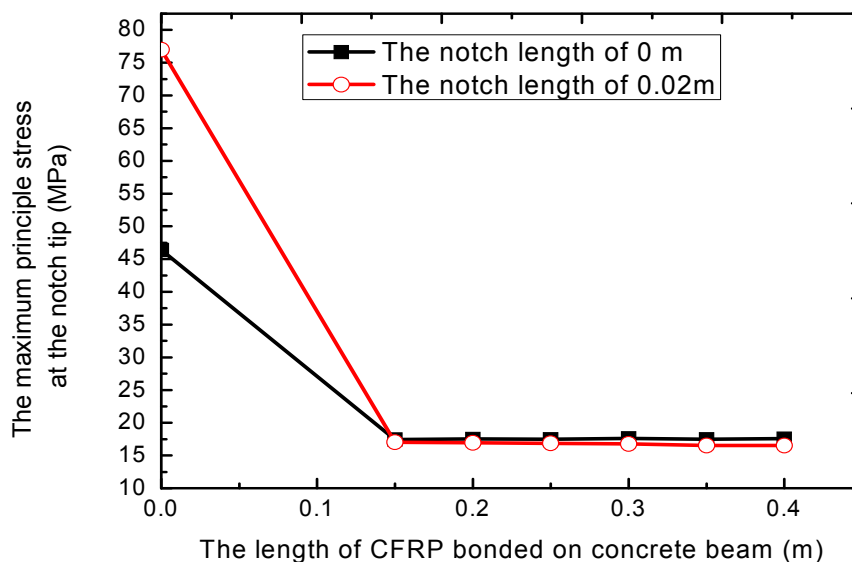


Figure 10 shows that CFRP bonded onto the bottom of a concrete beam can effectively prevent crack propagation for a notch tip in Mode I. Once the concrete beam is reinforced by CFRP, the stress concentration at the notch tip is significantly relieved, as indicated by the value of the maximum principal stress at the crack tip. The value for the stress decreased by 63% and 78% after concrete beam reinforcement with crack propagation lengths of 0 and 0.02 m, respectively. The reinforcement effect of CFRP on the concrete beam is prominent. When the CFRP length is 0 m to 0.15 m, the stress concentration of the notch tip deteriorates. However, when the length ranges between 0.15 m and 0.35 m, no influence of CFRP length on the value of the crack tip is observed. That is, within this length range, the influences of CFRP on the notch tip or the region around the crack tip are similar. If only the Type I crack propagation at the notch tip is considered while excluding the possibility of crack initiation and propagation at the bottom of the concrete specimen and at the end of the carbon fiber plate, the rigidity and the ultimate load of the RC beam will be improved with a 0.15 m length of CFRP.

### 3.2. The Effect of CFRP Length on Stresses at the Interface

This section discusses the effect of CFRP length on the stress field in concrete material at the root of the notch along the interface (marked as 2 in Figure 9). The size of the overstressed region was defined as the distance from the end point of the notch to the other point along the interface at which the stress exceeds the tensile strength of the concrete material. The magnitude of the size was taken as a parameter to measure how CFRP length influences the stress field. The size of the overstressed region is calculated when the lengths of the carbon fiber plate are 0.10 m, 0.15 m, 0.20 m, 0.25 m, 0.30 m, and 0.35 m for 0.02 m and 0 m notch lengths under 20 kN loading. Figure 11 plots the size of the overstressed region *versus* the length of CFRP.

**Figure 11.** The plot of the width of the overstressed region along the interface against the length of bonded CFRP.

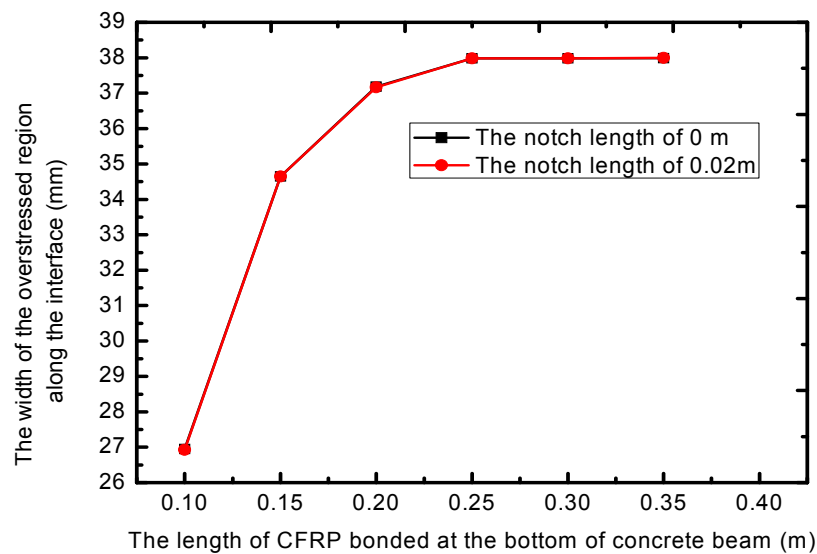


Figure 11 shows that with the Mode I crack propagation at the notch tip; the size of the overstressed region at the interface remains the same, which is consistent with the conclusion that the crack propagation at the notch tip has no effect on the overstressed region at the interface. The size of the overstressed region changes with the variation of CFRP length. The continually growing CFRP causes the overstressed region to exhibit an increasing tendency. Nevertheless, the size of the overstressed region at the interface does not change after the length of CFRP reaches a certain value. When the CFRP length reaches 0.20 m, the variation of the size of the overstressed region becomes less significant. When the CFRP length has reached 0.25 m, the size of the overstressed region at the interface will no longer be affected by the length of the carbon fiber plate.

### 3.3. The Effect of CFRP Length on Stresses at the End of CFRP

The influence of CFRP length on the local stress field at the end of CFRP is studied in this section, where the initial notch lengths are 0 and 0.02 m, and the concrete beams are strengthened with various CFRP lengths of 0.10 m, 0.20 m, 0.30 m and 0.35 m, respectively, subjected to a 20 kN load. In particular, the lengths of 0.15 m and 0.25 m are not chosen to be analyzed in this section, since 0.15 m is the optimum for affecting the stress distribution at the notch tip and 0.25 m the optimum length for the stress distribution along the interface. This section focuses on the trend excluding these two key lengths for the previous cases, while 0.35 m is close to the span length of the two supports of the concrete beam worthy of being solely studied. Such a procedure should be without loss of generality. The maximum principal stress in this region was also considered as a key parameter for studying the strengthening effects. Previous discussions [22,23] also showed that the tensile strength in the longitudinal direction of CFRP is significantly smaller than the tensile strength of 4640 MPa. Consequently, the strength of CFRP is not considered.

3.3.1. CFRP Length of 0.10 m

Figure 12 shows the distribution of the maximum principal stress in the concrete material at the end of CFRP when the CFRP length is 0.10 m under a 20 kN load. Figure 13 illustrates the specific values for the stresses around the region at the end of CFRP. If we define the length of the overstressed region as the distance along the interface between two nodes at which the maximum principal stresses are larger than the tensile stress of concrete material, 5.15 MPa, the value for the length reaches 25.61 mm in this case.

**Figure 12.** The distribution for the maximum principle stresses in concrete material at the end of CFRP with a length of 0.10 m.

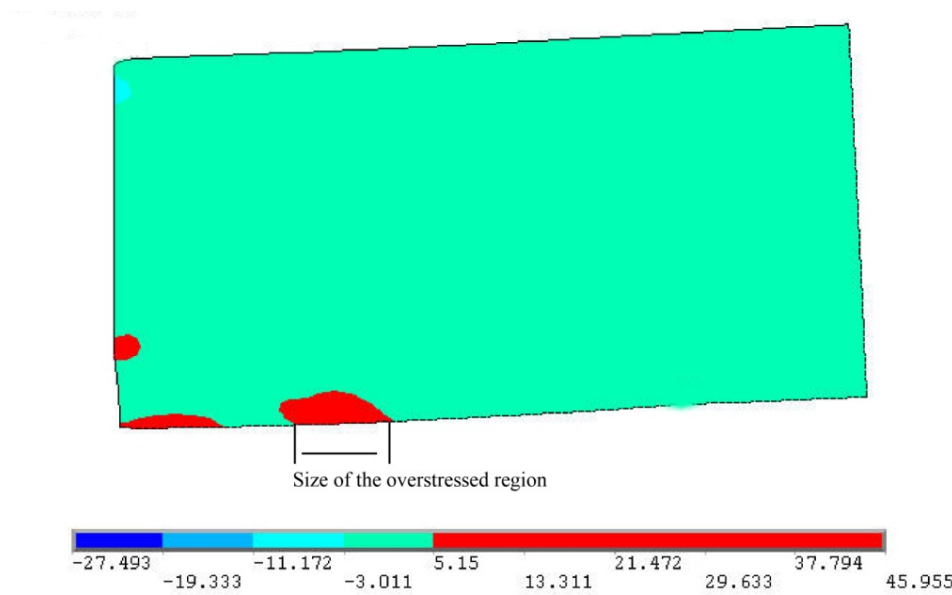


**Figure 13.** The specific value around the region at the end of the CFRP.

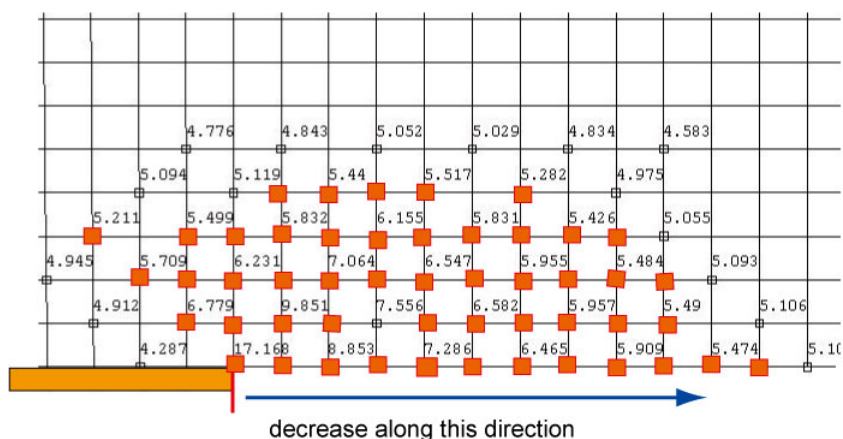


Figure 12 shows that the overstressed region of the concrete section at the end of the CFRP is clearly larger than that at the root of the notch along the interface. Figure 13 shows that starting from the end of the CFRP, the maximum principal stress of the concrete decreases along the interface until its value is less than the tensile strength of the concrete material. As load is applied to the CFRP-reinforced concrete beam, the initial crack (notch) initially extends in terms of the Mode I crack.

As the applied load increases, the initial crack propagates rapidly along the central line of the concrete beam. When the Type I crack extends to a certain length, the propagation will stop. Two other overstressed regions are formed along the interface between CFRP and the concrete beam, one located at the end of the CFRP and the other at the root of the notch on the interface, as illustrated in Figure 9. Owing to the CFRP restriction on the new crack initiated at the root of the notch, the increased load applied at the concrete beam is considerably sustained by the concrete at the end of the CFRP. Consequently, the second macroscopic crack after the initial crack at the crack tip will definitely appear at the end of the carbon fiber plate. The experimental observation in [23] also supports this finding. Subsequently, as the load is increased continually, the crack propagation at the end of the CFRP will gradually alleviate the reinforcement effect. The restriction of CFRP on the initial crack decreases and will continue to propagate as the load increases. Finally, the RC beam fails with the combination of the initial crack and the macroscopic crack at the end of CFRP. Hence, we can predict that when the CFRP length is less than or equal to 0.10 m, the macroscopic inclined crack at the end of the CFRP and the main crack will overlap with each other and then propagate together until the concrete beam fractures.

### 3.3.2. CFRP Length of 0.20 m

Figures 14 and 15 show the stress distribution for the maximum principal stresses in the concrete material at the end of the CFRP and the specific values for stresses when the CFRP length is 0.20 m under a 20 kN load. A comparison between Figures 12 and 14 shows that the overstressed region at the end of the CFRP shrinks to a small area as the CFRP length changes from 0.10 m to 0.20 m. This observation indicates that the stress concentration that occurred in the concrete material at the end of the CFRP has been significantly alleviated by the increased CFRP length. Figure 14 also illustrates that the size of the overstressed region at the end of the CFRP obviously decreased from 25.51 mm for the case of 0.10 m CFRP to 4.24 mm for the case of 0.20 m CFRP.

**Figure 14.** The distribution for the maximum principle stresses in concrete material at the end of CFRP with a length of 0.20 m.

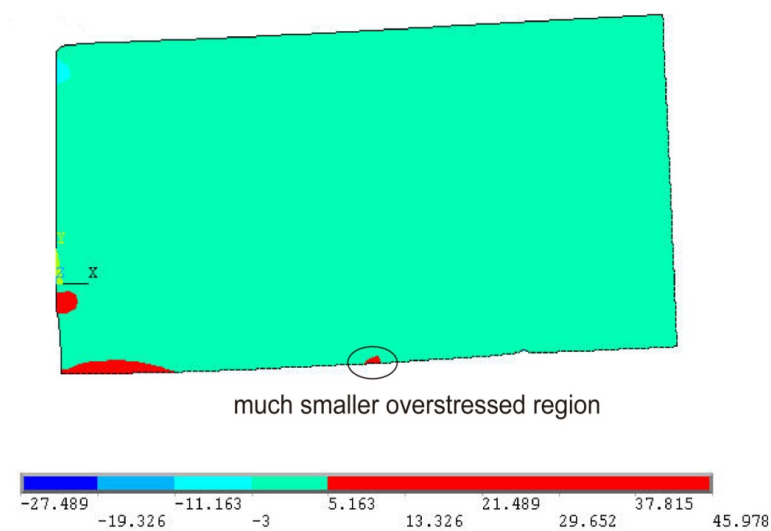
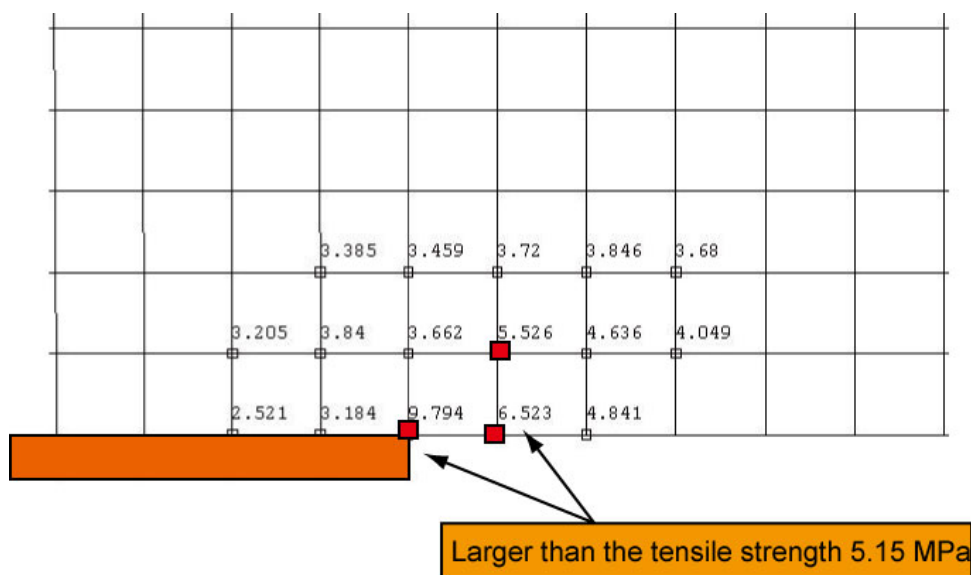


**Figure 15.** The specific value around the region at the end of the CFRP.



### 3.3.3. CFRP Length of 0.30 m

Similar to the discussion in previous sections, Figures 16 and 17 show the stress distribution for the maximum principal stresses in the concrete material at the end of CFRP and the specific values for these stresses when the CFRP length is 0.30 m under a 20 kN load. In both figures, the overstressed region (marked as red in Figures 16 and 17) can hardly be seen, which indicates that as the CFRP length increases, the stress concentration that developed in the concrete material at the end of the CFRP almost disappeared. However, the investigation on the stress values in this region, as illustrated in Figure 16, shows that a small region in which the values for stress exceed the tensile strength of concrete material exists. Measurement of the size of the overstressed area indicates that the size decreases to 1.35 mm, almost 1/24 of that of 0.10 m CFRP and a quarter of that of 0.20 m CFRP. Notably, the length of CFRP does not exceed the span of two concrete beam supports in this research for all cases. Although the overstressed region at the end of CFRP has shrunk and the stress concentration in this area is alleviated with the increase in CFRP length, the deflection of the RC beam and the tension in CFRP will become larger. Therefore, the shear stress that originated from the adhesive layer at the end of the CFRP will become more obvious. CFRP inhibits the propagation of the initial crack (notch). Thus, the failure of the RC beam is believed to be caused by the combination of the propagation of the inclined crack at 45° from the end of the CFRP and the propagation of the initial crack when the length of the CFRP is approximately 0.30 m.

**Figure 16.** The distribution for the maximum principle stresses in concrete material at the end of the CFRP with a length of 0.30 m.

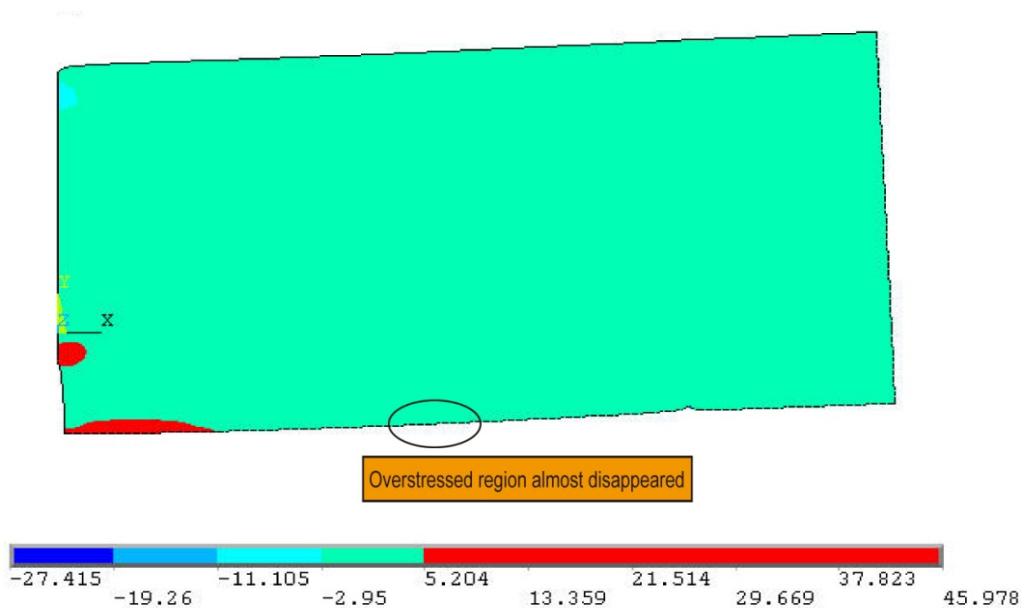
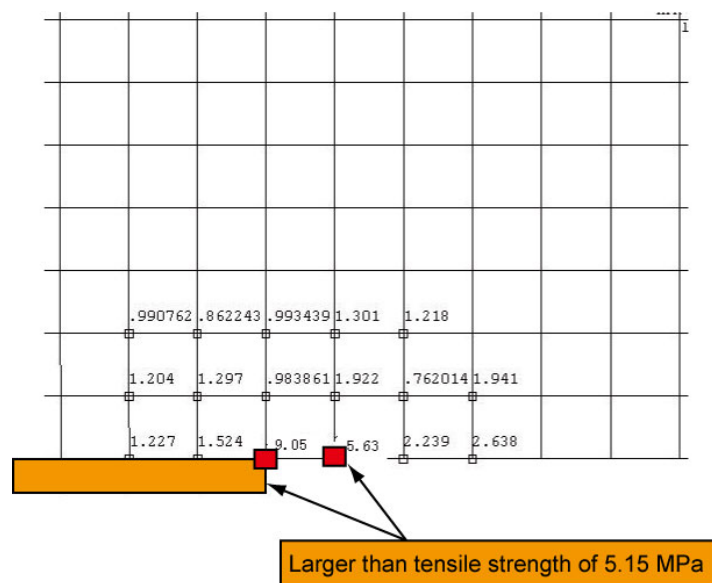


**Figure 17.** The specific value around the region at the end of the CFRP.



### 3.3.4. CFRP Length of 0.35 m

The CFRP length increases to 0.35 m, close to the span of the concrete beam at 0.40 m; the maximum principal stress in the concrete material at the end of CFRP is shown in Figure 18, and the details for stresses are illustrated in Figure 19. Figure 18 shows that the overstressed region at the end of the CFRP has completely disappeared. The specific values for the stresses, as shown in Figure 19, indicate that no values larger than the tensile strength of 5.15 MPa exist. The 0.35 m CFRP length completely alleviates the stress concentration at the end of the CFRP. However, this trend of disappearing concentration starts from the case of the 0.30 m CFRP length, which implies that concrete



concentration at the end of the CFRP. As the CFRP stretches continually, the maximum principal stresses that develop in the concrete section at the root of the notch increase, at the risk of rupture. A comparison between Figures 13 and 19 reveals that the size of this area markedly increased. Eventually, a smeared macro-crack originates and propagates along the interface, thus causing the delamination failure of the RC beam. The size of the overstressed region at the concrete section at the end of the CFRP will gradually be reduced to 0 mm with increasing CFRP length, thus reducing the possibility of concrete beam debonding failure at the end of the CFRP. However, the possibility of the failure at the root of the initial notch becomes increasingly larger. For the reinforced specimen studied in this work and subjected to 20 kN loading, the 0.30 m CFRP length is the optimum value at which CFRP strengthening is fully optimized on the concrete beam.

#### 4. Conclusions

Experiment measurements and FE analyses were performed on concrete beams strengthened with various lengths of CFRP bonded onto the bottom of a beam subjected to 20 kN loading applied to the central point. The following conclusions can be drawn:

- (1) The CFRP can significantly improve the load-bearing capacity for strengthened concrete beams.
- (2) The CFRP length can increase the ultimate load of the strengthened beam, while such an increase will stop as the CFRP length reaches 0.15 m.
- (3) The failure mode for strengthened concrete beams varies with CFRP length.
- (4) Three overstressed regions exist for the RC beams, one located at the tip of initial notch, the other at the root of the notch along the interface and the third at the end of the CFRP.
- (5) The values of the maximum principal stress in the concrete material at the end of the CFRP strongly depend on the CFRP length. However, the value remains the same when the CFRP length reaches a certain value at which it approaches the span of the RC beam. Meanwhile, the size of overstressed region exhibits a trend similar to that of stress.
- (6) When the CFRP length tends to 0.10 m, the overstressed region at the end of the carbon fiber plate becomes larger, and the stress concentration at the CFRP end becomes obvious. The failure mode in this case is dominated by the inclined crack at the end of the CFRP along with the Type I crack propagation at the initial crack (notch). When the CFRP length ranges from 0.10 m to 0.30 m, the overstressed region at the end of the CFRP decreases with the increase in the CFRP length, and the stress concentration at the plate end is alleviated. The failure mode in this case is a combination of the inclined crack at the CFRP end, the Type I crack at the initial notch and the smeared crack at the root of the notch along the interface. When the length of the CFRP is larger than 0.30 m, the stress concentration at the CFRP end disappears, but the stress at the root of the notch along the interface gradually increases, because of the tension in the CFRP. The failure mode in this case is dominated by the smeared crack propagation along the interface with the Type I crack at the initial notch.

#### Acknowledgments

This work is financially supported by the Natural Science Foundation of China (11302272), by the Natural Science Foundation of China (11272368), by the 2013 Program for Innovation Team Building

at Institutions of Higher Education in Chongqing (KJTD201319) and by the Science and Technology Project Affiliated with the Education Department of Chongqing Municipality (KJ120801).

### Author Contributions

Jun Ding is responsible for performing the numerical simulation and has contributed to the writing of all the sections within paper. Fang Wang is working on experimental measurement and has been in charge of writing the sections regarding test. Xia Huang is responsible for theoretical derivation on ultimate load. Song Chen is responsible for the research project.

### Conflicts of Interest

The authors declare no conflict of interest.

### References

1. Anwarul Islam, A.K.M. Effective methods of using CFRP bars in shear strengthening of concrete girders. *Eng. Struct.* **2009**, *31*, 709–714.
2. Biscaia, H.C.; Chastre, C.; Silva, M.A. Nonlinear numerical analysis of the debonding failure process of FRP-to-concrete interfaces. *Compos. B Eng.* **2010**, *50*, 210–223.
3. Michels, J.; Christen, R.; Waldmann, D. Experimental and numerical investigation on postcracking behavior of steel fiber reinforced concrete. *Eng. Fract. Mech.* **2013**, *98*, 326–349.
4. Sundararaja, M.C.; Rajamohan, S. Strengthening of RC beams in shear using GFRP inclined strips—An experimental study. *Construct. Build. Mater.* **2009**, *23*, 856–864.
5. Edberg, W.; Mertz, D.; Gillespie, J., Jr. Rehabilitation of steel beams using composites materials. In Proceedings of ASCE Fourth Material Engineering Conference, Washington, D.C., USA, 10–14 November 1996; pp. 502–508.
6. Buyle-Bodin, F.; David, E.; Ragneau, E. Finite element modelling of flexural behaviour of externally bonded CFRP reinforced concrete structures. *Eng. Struct.* **2002**, *24*, 1423–1429.
7. Mazzotti, C.; Savoia, M.; Ferracuti, B. An experimental study on delamination of FRP plates bonded to concrete. *Constr. Build. Mater.* **2008**, *22*, 1409–1421.
8. Martinez, X.; Oller, S.; Rastellini, F.; Barbat, A. A numerical procedure simulating RC structures reinforced with FRP using the serial/parallel mixing theory. *Comput. Struct.* **2008**, *86*, 1604–1618.
9. Tavakkolizadeh, M.; Saadatmanesh, H. Fatigue strength of steel girders strengthened with carbon fiber reinforced polymer patch. *J. Struct. Eng.* **2003**, *129*, 186–196.
10. Xue, W.; Zeng, L.; Tan, Y. Experimental studies on bond behavior of high strength CFRP plates. *Compos. B Eng.* **2008**, *39*, 592–603.
11. Valivonis, J.; Skuturna, T. Cracking and strength of reinforced concrete structures in flexure strengthened with carbon fibre laminates. *J. Civ. Eng. Manag.* **2007**, *4*, 317–323.
12. Deng, J.; Lee, M.M.K.; Moy, S.S.J. Stress analysis of steel beams reinforced with a bonded CFRP plate. *Compos. Struct.* **2004**, *65*, 205–215.

13. Buyukozturk, O.; Gunes, O.; Karaca, E. Progress on understanding debonding problems in reinforced concrete and steel members strengthened using FRP composites. *Constr. Build. Mater.* **2004**, *18*, 9–19.
14. Schnerch, D.; Stanford, K.; Sumner, E.; Rizkalla, S. Bond behavior of CFRP strengthened steel bridges and structures. In Proceedings of International Symposium on Bond Behavior of FRP in Structures, Hong Kong, China, 7–9 December 2005.
15. Schnerch, D.; Dawood, M.; Rizkalla, S.; Sumner, E.; Stanford, K. Bond behavior of CFRP strengthened steel structures. *Adv. Struct. Eng.* **2006**, *9*, 805–817.
16. Colombi, P. Reinforcement delamination of metallic beams strengthened by FRP strips: Fracture mechanics based approach. *Eng. Fract. Mech.* **2006**, *73*, 1980–1995.
17. Belachour, A.; Benyoucefa, S.; Tounsi, A.; Adda bedia, E.A. Interfacial stress analysis of steel beams reinforced with bonded prestressed FRP plate. *Eng. Struct.* **2008**, *30*, 3305–3315.
18. Al-Emarani, M.; Kliger, R. Experimental and numerical investigation of the behavior and strength of composite steel-CFRP members. *Adv. Struct. Eng.* **2006**, *9*, 819–831.
19. Lu, X.Z.; Jiang, J.J.; Teng, J.G.; Ye, L.P. Finite element simulation of debonding in FRP-to-concrete bonded joints. *Constr. Build. Mater.* **2006**, *20*, 412–424.
20. Atas, A.; Soutis, C. Strength prediction of bonded joints in CFRP composite laminates using cohesive zone elements. *Compos. B Eng.* **2014**, *58*, 25–34.
21. Chen, G.M.; Chen, J.F.; Teng, J.G. On the finite element modelling of RC beams shear strengthened with FRP. *Constr. Build. Mater.* **2012**, *32*, 13–26.
22. Ding, J. Crack failure study of CFRP reinforced concrete beams. Master Thesis, Chongqing University, Chongqing, China, 1 July 2004.
23. Niu, S.S. The experimental study on concrete beams strengthened with CFRP. Master Thesis, Chongqing University, Chongqing, China, 1 July 2002.
24. Ding, J.; Huang, X.; Zhu, G.; Chen, S.; Wang, G.C. Mechanical performance evaluation of concrete beams strengthened with CFRP. *Adv. Mater. Sci. Eng.* **2013**, *2013*, 1–9.
25. *Concrete Structure Design Specifications*; GB50010-2010; China Building Industry Press: Beijing, China, 2011.
26. *Product Specifications for CFRP*; Taiwan Zhongyi Company Press: Taiwan, 2012.
27. Chinese Aeronautical Establishment. *The Handbook for Stress Intensity Factors*; Beijing Science Press: Beijing, China, 1981.
28. ABAQUS, version 6.10; User Documentation; Dassault Systemes: Vélizy-Villacoublay, France, 2010.